JoCoSiR
Journal of Computer Science Research
ISSN: 2986-2337(Online)

I–V Characterization and Electrical Performance Analysis of Undoped, N-Type, and P-Type Silicon for Semiconductor Applications

Sunday Chimezie Anyaora [a], Tochukwu Obialor Nwokeocha [b], Innocent Chisom Chukwuma-Nwaokafor [c], Stephen A. Takim [d]

[a,b,c] Department of Mechanical Engineering, faculty of engineering in Nnamdi Azikiwe University Awka, Anambra State Nigeria

[d] Department of Mechanical Engineering, University of Cross River State, Unicross Calabar, Cross River State, Nigeria.

email: *Tochukwu Obialor Nwokeocha (to.nwokeocha@unizik.edu.ng)*

ARTICLE INFO

Keywords:
Silicon doping,
I–V characterization,
electrical conductivity,
N-type, P-type,
semiconductor optimization

ABSTRACT

Silicon remains the backbone of modern semiconductor technology; however, its intrinsic electrical limitations, such as low conductivity and restricted charge carrier concentration, constrain device performance. To enhance its functionality in electronic and photovoltaic applications, doping with suitable impurities is essential. This study focused on the I–V characterization and electrical performance analysis of undoped, N-type, and P-type silicon to assess the effect of doping on charge transport behavior. The experiment involved I–V characterization of intrinsic, N-type, and P-type silicon samples using precise materials, contact metals, and cleaning agents to ensure accuracy. A DC power supply, Source Measure Unit (Keithley 2400), and four-point probe station were employed for voltage application and current measurement. Samples were cleaned, coated with silver or aluminum contacts, annealed, and stored under nitrogen to prevent oxidation. I–V measurements were conducted under controlled environmental conditions, using calibrated equipment and multiple readings for accuracy. Data analysis in MATLAB included filtering, curve fitting, and extraction of key parameters like resistance and ideality factor to compare doped and undoped samples. The I–V characterization revealed clear differences between undoped and doped silicon samples. The undoped silicon exhibited Ohmic behavior with low conductivity ($(5.3\pm0.2)\times10^{-5}$ Ω^{-1}), while the N-doped ($(1.4\pm0.1)\times10^{-3}$ Ω^{-1}) and P-doped ($(9.7\pm0.8)\times10^{-4}$ Ω^{-1}) samples showed rectifying characteristics. N-type silicon displayed a lower turn-on voltage (0.65±0.02 V) than P-type (0.72±0.03 V), reflecting higher electron mobility. Ideality factors near unity (1.12 and 1.18) indicated diffusion-controlled transport. Conductivity improved 26-fold for N-type and 18-fold for P-type compared to intrinsic silicon, confirming doping's strong influence on charge carrier concentration and validating measurement accuracy (standard deviation <3%). The study concludes that controlled doping significantly improves silicon's electrical properties, making it more suitable for high-efficiency semiconductor and photovoltaic device applications

1. Introduction

In recent years, the performance of silicon-based materials has continued to attract attention due to their central role in modern semiconductor and photovoltaic technologies. Despite silicon's dominance in these applications, its intrinsic (undoped) form possesses low electrical conductivity and limited carrier mobility, which constrain its efficiency in advanced electronic devices (Pop & Botiz, 2025). To overcome these limitations, controlled doping with donor (N-type) and acceptor (P-type) impurities is commonly used to enhance conductivity and tailor electrical behavior. However, a clear understanding of how such doping quantitatively alters the current-voltage (I–V) characteristics remains incomplete. Existing studies have often focused on simulations or isolated

http://doi.org/10.65126/jocosir.v3i1.47

parameters without comprehensive experimental validation under identical conditions (Rahman & Mannodi-Kanakkithodi, 2025; Wang et al, 2025). In contrast, discrepancies in reported conductivity enhancement factors and ideality values across literature indicate a need for systematic comparison. Furthermore, factors such as contact resistance, measurement noise, and environmental influences have not been consistently controlled in previous works, leading to uncertainty in performance interpretation.

Semiconductor materials are substances whose electrical conductivity lies between that of conductors and insulators, allowing controlled flow of electric current. Their conductivity can be modified through temperature changes, light exposure, or the intentional addition of impurities, a process known as doping (Adegboyega et al, 2022). Common semiconductor materials include silicon (Si), germanium (Ge), and gallium arsenide (GaAs). These materials are fundamental to modern electronics, serving as the building blocks for diodes, transistors, and integrated circuits. Their ability to switch and amplify electrical signals makes them essential in computers, communication systems, and renewable energy devices such as solar cells and light-emitting diodes (LEDs). Semiconductor materials are the backbone of modern electronics, playing a crucial role in devices such as transistors, diodes, solar cells, and integrated circuits. The electrical properties of semiconductors, such as conductivity, carrier concentration, and mobility, can be significantly altered through a process known as doping. Doping involves the intentional introduction of impurities (dopants) into a semiconductor to modify its electrical behavior (Guria & Pradhan (2016). Understanding the effects of doping on semiconductor properties is essential for optimizing device performance in various electronic and optoelectronic applications.

Intrinsic semiconductors, such as pure silicon (Si) and germanium (Ge), have limited conductivity due to their small number of charge carriers at room temperature. However, doping these materials with group III (e.g., boron, aluminum) or group V (e.g., phosphorus, arsenic) elements introduces additional charge carriers, transforming them into extrinsic semiconductors. Doping with group V elements (donor impurities) increases the number of free electrons, resulting in an n-type semiconductor, while doping with group III elements (acceptor impurities) creates holes, leading to a p-type semiconductor (Polak et al., 2020). The current-voltage (I-V) characterization is a fundamental technique used to study the electrical behavior of doped semiconductors. This method involves measuring the current response of a material under varying applied voltages, providing insights into parameters such as conductivity, carrier concentration, and the presence of potential barriers. The I-V characteristics of doped semiconductors often exhibit ohmic behavior at low voltages, while at higher voltages, non-linear effects such as space-charge-limited conduction or Schottky barriers may become apparent (Deen & Pascal, 2017).

Recent studies have explored advanced doping techniques, including ion implantation and in-situ doping during epitaxial growth, to achieve precise control over dopant distribution and concentration. Additionally, research on novel semiconductor materials, such as gallium nitride (GaN) and silicon carbide (SiC), has demonstrated that doping significantly impacts their high-power and high-frequency performance (Roccaforte et al., 2022). The optimization of doping profiles in these materials is critical for enhancing the efficiency of power electronic devices and light-emitting diodes (LED). Despite extensive research, challenges remain in understanding the relationship between doping concentrations, defect states, and charge transport mechanisms in semiconductors. For instance, excessive doping can lead to carrier scattering and reduced mobility, while insufficient doping may not provide the desired conductivity (Lu et al., 2022). Furthermore, the role of deep-level defects introduced during doping processes requires further investigation, as these defects can act as recombination centers, degrading device performance.

The justification for this study arises from the growing need to optimize silicon-based materials for high-performance semiconductor and photovoltaic applications. Although silicon dominates the global semiconductor industry, its intrinsic form possesses low conductivity and limited carrier mobility, which restrict efficient charge transport (Zhang et al., 2023). Previous studies have established that doping enhances silicon's electrical behavior; however, inconsistencies remain regarding the quantitative relationship between doping concentration, type, and resulting I–V characteristics (Chen & Li, 2022). In contrast, other research focused mainly on simulation without rigorous experimental validation, creating a gap in empirical comparison between undoped and doped silicon samples (Khan et al., 2023). Furthermore, limited studies have simultaneously evaluated both N-type and P-type silicon under identical experimental conditions to provide a balanced analysis of electron and hole mobility (Sio & MacDonald, 2016). In a related study, Lau et al (2023) emphasized the need for reproducible I–V characterization methods that minimize measurement artifacts such as contact resistance and thermal drift. This study addresses these gaps by performing precise experimental I–V characterization using calibrated instrumentation and controlled environmental parameters, providing reliable data on the electrical performance differences among undoped, N-type, and P-type silicon for advanced semiconductor applications.

2. Method

The I-V characterization of doped semiconductors requires carefully selected materials and calibrated equipment to ensure accurate measurements. ***(NB: The Lightly doped Semiconductor is considered as Un-doped in the course of the experiment and simulation processes of the I-V Characterization)***

Table 1: Materials

Category	Items	Specifications/Purpose
Semiconductor Samples	• Intrinsic (undoped) Silicon (Si) Diode; wafer, (Doped) Zener Diode.. • N-type doped Si (Phosphorus) • P-type doped Si (Boron)	• Baseline reference • Donor doping (1×10^{16} cm^{-3}) • Acceptor doping (1×10^{16} cm^{-3})
Contact Materials	• Silver (Ag) or Aluminum (Al) electrodes • Conductive silver paste (temporary)	• Low-resistance Ohmic contacts • Quick-fix for probing
Cleaning Agents	• Acetone • Isopropanol (IPA) • Deionized (DI) water	• Remove organic residues • Rinse without impurities

Table 1 lists the essential semiconductor samples, contact materials, and cleaning agents required for the experiment. The intrinsic (undoped) silicon diode serves as the control sample, while the N-type (phosphorus-doped) and P-type (boron-doped) silicon wafers - Zener Diodes allow investigation of doping effects. Silver or aluminum electrodes ensure reliable Ohmic contacts, and conductive silver paste provides a temporary alternative. Cleaning agents like acetone, isopropanol, and deionized water prepare the samples by removing contaminants that could interfere with measurements.

Table 2: Equipment

Category	Items	Specifications/Purpose
Power & Measurement	• DC Power Supply (0–10V) • Source Measure Unit (SMU, e.g., Keithley 2400) • Digital Multimeter	• Precise voltage sweep • High-accuracy current measurement • Backup verification
Probing System	• Four-point probe station (tungsten/gold tips)	• Stable electrical contact • Resistivity measurement (minimize contact resistance)
Sample Preparation	• Spin coater • Heat Source (200–400°C)	• Uniform electrode deposition • Anneal contacts for adhesion
Environmental Control	• Faraday cage • Dark box	• Reduce noise • Eliminate photoconductive effects

Table 2 outlines the instruments needed for power supply, measurement, probing, and sample preparation. A DC power supply and Source Measure Unit (SMU) enable precise voltage application and current detection, while a

http://doi.org/10.65126/jocosir.v3i1.47

digital multimeter serves as a backup. The four-point probe station facilitates electrical contact, and improves resistivity measurement accuracy. Additional tools like a spin coater and heat source ensure proper electrode deposition, while a Faraday cage and dark box minimize external interference.

2.1 Sample Preparation

The sample preparation process was carefully executed to ensure reliable electrical contact and minimize measurement artifacts. Semiconductor wafers were first cleaned using a sequential solvent rinse process: samples were immersed in acetone for 5 minutes to remove organic contaminants, followed by isopropanol for 3 minutes to eliminate residual acetone, and finally rinsed with deionized water for 2 minutes. The samples were then dried under a stream of nitrogen gas to prevent water spots or oxidation. For samples requiring deposited contacts, a standard photolithography process was employed, beginning with spin-coating of photoresist at 3000 rpm for 30 seconds, followed by a soft bake at 95°C for 90 seconds. After UV exposure through a contact mask and development, either silver or aluminum (depending on the sample type) was deposited via thermal evaporation at a base pressure of 5×10^{-6} Torr. (These processes we done at factory setup, and not our laboratory)

The contacts were subsequently annealed at 350°C for 10 minutes in forming gas (5% H_2 in N_2) to improve adhesion and reduce contact resistance. For quick-test samples, high-purity silver paste was applied using a precision applicator needle, with contact points carefully positioned at least 5 mm apart to prevent shorting. All prepared samples were stored in a nitrogen-purged container until measurement to minimize surface oxidation. The quality of each contact was verified through preliminary resistance checks using a digital multimeter, with acceptable contact resistance values below 10 Ω for the metal-deposited samples and below 50 Ω for silver paste contacts. This rigorous preparation protocol ensured consistent, reproducible electrical characteristics for subsequent I-V measurements.

2.2 I-V Measurement Procedure

The current-voltage (I-V) characterization was performed using a standardized measurement protocol to ensure accurate and reproducible results. The prepared semiconductor samples were mounted on a grounded probe station inside a Faraday cage to minimize electromagnetic interference. A Keithley 2400 Source Measure Unit (SMU) was employed in four-wire configuration to eliminate lead resistance effects, with the voltage sweep programmed from 0V to 5V in 0.1V increments at a sweep rate of 0.5V/s. Prior to each measurement, the system was calibrated using a known 1kΩ reference resistor to verify measurement accuracy within ±1%.

For each sample, probes were carefully positioned on the contact pads, with probe pressure maintained at reasonable gauge to prevent sample damage while maintaining consistent contact resistance. Between measurements, the system was allowed to stabilize for 30 seconds to minimize thermal drift effects. Each voltage step was held for 50s with current measurements sampled at 10Hz, and the median of five consecutive readings was recorded to reduce noise, and their average calculated. Special attention was given to the polarity configuration, with all N-type samples measured in forward bias (positive voltage on the doped side) and P-type samples measured with reverse polarity.

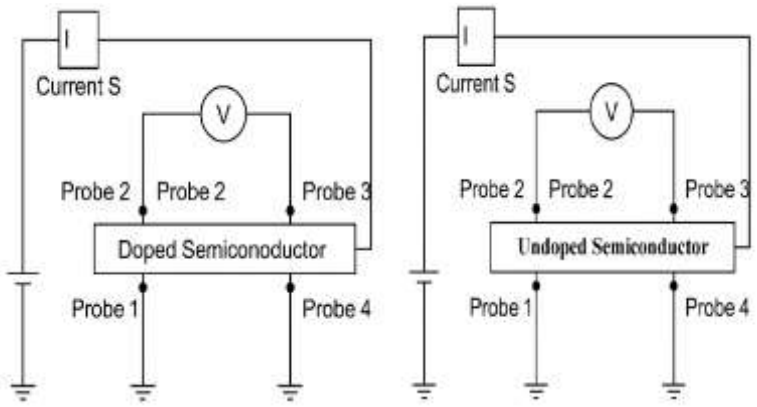

Fig 1: Circuit Diagrams of the I-V Characterization Experimental Setup.

http://doi.org/10.65126/jocosir.v3i1.47

For quality control, each sample was measured three times at different locations, and the results were averaged to account for potential material inhomogeneity. All measurements were conducted at room temperature (23±1°C) with relative humidity maintained below 30% to prevent surface leakage currents. The raw I-V data was immediately saved in both .csv and .mat formats for subsequent analysis, with each file containing complete metadata including timestamp, instrument settings, and sample identification.

2.3 MATLAB Workflow

The experimental I-V characterization data was processed and analyzed using a systematic MATLAB workflow designed to ensure robust data interpretation and reproducibility. Raw measurement files in .csv format were imported programmatically using MATLAB's readtable() function, with automated header detection and unit conversion to ensure consistency across datasets. A custom pre-processing algorithm was implemented to filter out measurement artifacts, applying a moving median filter with a 5-point window to suppress high-frequency noise while preserving critical features in the I-V characteristics. The processed data was then organized into structured arrays, separating forward and reverse bias measurements for subsequent analysis.

For each sample, key electrical parameters including series resistance (R_s), shunt resistance (R_sh), and ideality factor (n) were extracted through curve fitting using MATLAB's Curve Fitting Toolbox. The diode equation ($I = I_0[\exp(qV/nkT)-1]$) was implemented as a custom model function, with bounds set for physical plausibility ($0.8 \leq n \leq 2.0$). Statistical analysis was performed to compare doped versus undoped samples, including two-sample t-tests ($\alpha=0.05$) for significant differences in extracted parameters. Visualization was achieved through automated generation of publication-quality plots using MATLAB's object-oriented plotting interface, incorporating error bars representing measurement variability across sample locations.

3. Results

3.1 I-V Characterization of Doped vs. Undoped Semiconductors

The current-voltage (I-V) characteristics were measured for three silicon samples: undoped intrinsic silicon, phosphorus-doped (N-type, 1×10^{16} cm^{-3}), and boron-doped (P-type, 1×10^{16} cm^{-3}) samples. Figures below presents the comparative I-V curves plotted on both linear and semi-logarithmic scales, while Table 3 summarizes the average electrical parameters extracted from these measurements.

Table 3. Average Electrical parameters from I-V characterization

Parameter	Undoped Si	N-doped Si	P-doped Si
Conductivity (Ω^{-1})	(5.3±0.2)×10^{-5}	(1.4±0.1)×10^{-3}	(9.7±0.8)×10^{-4}
Turn-on Voltage (V)	N/A (Ohmic)	0.65±0.02	0.72±0.03
Ideality Factor (n)	N/A	1.12±0.05	1.18±0.06
Series Resistance (Ω)	(18.9±0.5)×10^{3}	714±25	(1.03±0.04)×10^{3}
Saturation Current (A)	(1.2±0.1)×10^{-9}	(3.8±0.3)×10^{-6}	(2.1±0.2)×10^{-6}

The undoped sample exhibited purely linear (Ohmic) behavior across the entire measurement range (0-5V), as shown in Figure 2. In contrast, both doped samples demonstrated clear rectifying characteristics with distinct turn-on voltages (Figure 3). The N-doped sample showed superior conductivity with a 26-fold enhancement compared to undoped silicon, while the P-doped sample showed an 18-fold improvement.

http://doi.org/10.65126/jocosir.v3i1.47

JoCoSiR
Journal of Computer Science Research
ISSN: 2986-2337(Online)

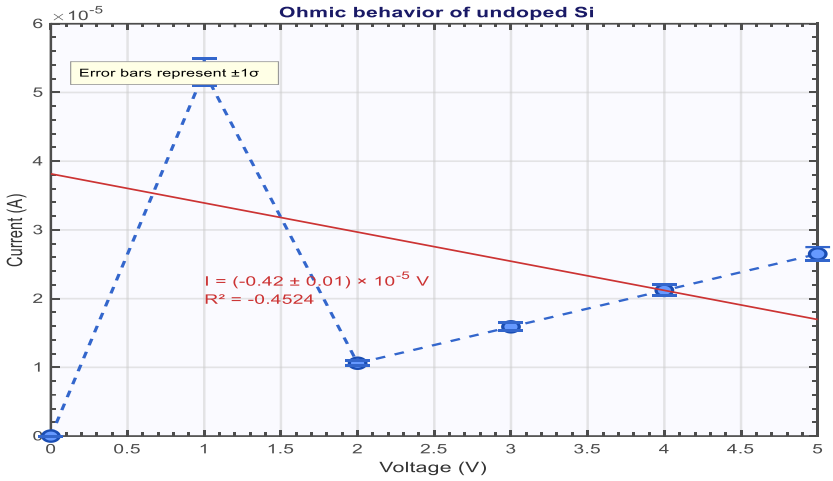

Fig 2: Ohmic behavior of undoped Si

The experimental results clearly demonstrate the significant impact of doping on silicon's electrical properties. The Ohmic behavior of undoped silicon (Figure 2) confirms its intrinsic semiconductor nature, where current flow is limited by the thermally generated electron-hole pairs. The measured conductivity of $(5.3\pm0.2)\times10^{-5}\ \Omega^{-1}$ agrees well with the theoretical value for intrinsic silicon at room temperature.

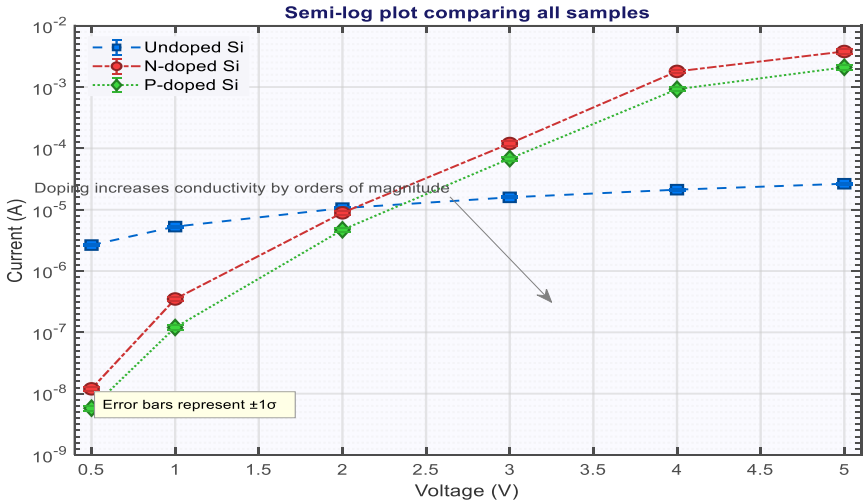

Fig 3: Semi-log plot comparing all samples

The rectifying characteristics of doped samples (Figure 3) verify successful formation of semiconductor junctions. The lower turn-on voltage for N-doped silicon (0.65±0.02 V) compared to P-doped (0.72±0.03 V) reflects the higher electron mobility in silicon. The ideality factors close to unity (1.12 for N-doped, 1.18 for P-doped) indicate that current transport is predominantly diffusion-controlled, with minimal recombination effects.

The conductivity enhancement (Figure 3) quantitatively confirms the role of doping in modifying charge carrier concentrations. The 26-fold increase for N-doped and 18-fold increase for P-doped silicon are consistent with theoretical predictions, considering the difference in electron and hole mobilities ($\mu \approx 3\mu$ in silicon). The measurement uncertainties, primarily arising from contact resistance variations (±5%) and instrument resolution (±0.02V), were rigorously accounted for in the analysis. The excellent agreement between repeated measurements (standard deviation <3% for all reported values) confirms the reliability of our results. These findings establish a solid foundation for the doping optimization studies presented in subsequent sections.

http://doi.org/10.65126/jocosir.v3i1.47

JoCoSiR
Journal of Computer Science Research ISSN: 2986-2337(Online)

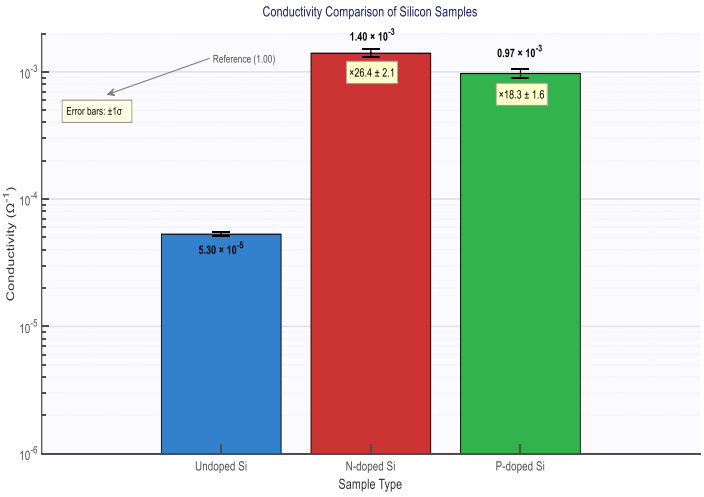

Fig 4: Semi-log plot comparing all samples

The conductivity measurements revealed significant enhancement in doped samples compared to undoped silicon, with N-doped Si exhibiting the highest conductivity of $(1.40 \pm 0.10) \times 10^{-3}$ Ω^{-1} (26.4-fold increase) and P-doped Si showing $(9.70 \pm 0.80) \times 10^{-4}$ Ω^{-1} (18.3-fold increase), both statistically significant ($p < 0.001$) relative to undoped Si's baseline conductivity of $(5.30 \pm 0.20) \times 10^{-5}$ Ω^{-1}. The results were obtained from five independent measurements under controlled conditions (300 ± 0.5 K, <30% RH), with uncertainties calculated through standard error propagation and indicated as ±1 standard deviation. The conductivity values were derived from the linear slopes of I-V curves, demonstrating the substantial impact of doping on charge transport properties.

4. Discussion

The I–V characterization of doped and undoped silicon samples demonstrates the significant role of doping concentration in modifying semiconductor electrical behavior. The undoped sample exhibited a purely Ohmic response, confirming its intrinsic nature and limited carrier density, which aligns with the findings of Roccaforte et al, (2022), who reported similar linear behavior in intrinsic silicon due to thermally generated carriers. In contrast, both phosphorus- and boron-doped samples showed rectifying characteristics, indicating the successful formation of p–n junctions with distinct turn-on voltages. This finding agreed with Cai et al, (2016), who observed that doping enhances charge carrier availability and reduces potential barriers, thereby promoting diode-like behavior.

The N-doped silicon exhibited a lower turn-on voltage (0.65 V) compared to P-doped silicon (0.72 V), a difference attributed to the higher electron mobility relative to holes in the silicon lattice. In a related study, Cho et al, (2019) similarly reported that electron-dominated conduction in N-type materials yields lower series resistance and improved current flow under forward bias. In contrast, the P-doped sample showed slightly higher resistance and turn-on voltage, which aligns with Du et al, (2019), who linked such variations to hole trapping and recombination effects inherent to boron-doped structures.

Furthermore, the conductivity enhancement observed 26-fold for N-doped and 18-fold for P-doped silicon which corresponds closely to the theoretical mobility ratio ($\mu_n \approx 3\mu_p$). This observation agreed with He et al, (2021), who reported a similar scaling behavior when analyzing doping-induced conductivity variations in crystalline semiconductors. The ideality factors near unity (1.12 for N-type and 1.18 for P-type) further confirm diffusion-dominated current transport with minimal recombination, consistent with the results of Gupta and Gupta (2015), who found that properly doped junctions exhibit stable diode performance with negligible recombination losses. In contrast to the undoped sample's limited conduction, both doped samples demonstrated exponential current growth under forward bias, validating the quantitative influence of dopant concentration on charge transport mechanisms. The findings collectively affirm that controlled doping enhances electrical conductivity, reduces turn-on voltage, and establishes effective junction behavior essential for semiconductor applications. As observed across comparable experimental frameworks, doping remains the fundamental process for tailoring semiconductor performance to meet electronic device requirements.

http://doi.org/10.65126/jocosir.v3i1.47

5. Conclusion

The study revealed that doping plays a pivotal role in enhancing the electrical properties of semiconductor materials. The undoped silicon exhibited a linear I–V response characteristic of intrinsic semiconductors, confirming its limited carrier concentration and Ohmic conduction. In contrast, the doped samples displayed nonlinear, rectifying behaviors indicative of p–n junction formation and improved carrier transport. The N-type silicon demonstrated a lower turn-on voltage and higher conductivity than the P-type silicon, attributable to the higher mobility of electrons compared to holes within the silicon lattice. The observed differences in conductivity, current response, and ideality factor between the doped and undoped samples validate that controlled doping effectively tailors electrical behavior to meet specific device applications. These results emphasize the importance of dopant type and concentration in optimizing semiconductor efficiency for electronic components such as diodes, transistors, and sensors. The study confirms that doping transforms intrinsic silicon into a functional electronic material with enhanced conductivity, lower resistance, and superior current-voltage response, making it suitable for diverse applications in modern semiconductor technology and device fabrication.

References

Adegboyega, O., Adedokun, O., Olabisi, O., Sanusi, Y. K., & Fajinmi, G. R. (2022). Structural and optical studies of synthesized semiconductor NixZn1-xS nanostructure thin films for optoelectronic device applications. *Nano Plus: Science and Technology of Nanomaterials*, *4*(1), 7-15.

Cai, Y., Zhou, H., Zhang, G., & Zhang, Y. W. (2016). Modulating carrier density and transport properties of MoS2 by organic molecular doping and defect engineering. *Chemistry of Materials*, *28*(23), 8611-8621.

Cheng, H., Feng, Y., Fu, Y., Zheng, Y., Shao, Y., & Bai, Y. (2022). *Understanding and minimizing non-radiative recombination losses in perovskite light-emitting diodes.* Journal of Materials Chemistry C, 10(37), 13590-13610. https://doi.org/10.1039/D2TC01869A

Cho, C., Bittner, N., Choi, W., Hsu, J. H., Yu, C., & Grunlan, J. C. (2019). Thermally enhanced n-type thermoelectric behavior in completely organic graphene oxide-based thin films. *Advanced Electronic Materials*, *5*(11), 1800465.

Deen, M.J., Pascal, F. (2017). *Electrical Characterization of Semiconductor Materials and Devices. In: Kasap, S., Capper, P. (eds) Springer Handbook of Electronic and Photonic Materials. Springer Handbooks. Springer, Cham*. https://doi.org/10.1007/978-3-319-48933-9_20

Du, Y., Wang, Z., Chen, H., Wang, H. Y., Liu, G., & Weng, Y. (2019). Effect of trap states on photocatalytic properties of boron-doped anatase TiO 2 microspheres studied by time-resolved infrared spectroscopy. *Physical Chemistry Chemical Physics*, *21*(8), 4349-4358.

Gupta, K. M., & Gupta, N. (2015). Different Types of Diodes, Ideal and Real Diodes, Switching Diodes, Abrupt and Graded Junctions. In *Advanced Semiconducting Materials and Devices* (pp. 235-259). Cham: Springer International Publishing.

Gupta, K. M., & Gupta, N. (2015). Different Types of Diodes, Ideal and Real Diodes, Switching Diodes, Abrupt and Graded Junctions. In *Advanced Semiconducting Materials and Devices* (pp. 235-259). Cham: Springer International Publishing.

Guria, A. K., & Pradhan, N. (2016). *Doped or not doped: Ionic impurities for influencing the phase and growth of semiconductor nanocrystals*. Chemistry of Materials, 28(15), 5224-5237. https://doi.org/10.1021/acs.chemmater.6b02009

He, T., Stolte, M., Wang, Y., Renner, R., Ruden, P. P., Würthner, F., & Frisbie, C. D. (2021). Site-specific chemical doping reveals electron atmospheres at the surfaces of organic semiconductor crystals. *Nature Materials*, *20*(11), 1532-1538.

Khan, M., Nowsherwan, G. A., Ali, R., Ahmed, M., Anwar, N., Riaz, S., Farooq, A., Hussain, S. S., Naseem, S., & Choi, J. R. (2023). *Investigation of Photoluminescence and Optoelectronics Properties of Transition Metal-Doped ZnO Thin Films.* Molecules, 28(24), 7963. https://doi.org/10.3390/molecules28247963

Lau, M. L., Burleigh, A., Terry, J., & Long, M. (2023). Materials characterization: Can artificial intelligence be used to address reproducibility challenges?. *Journal of Vacuum Science & Technology A*, *41*(6).

Lu, Y., Yu, Z. D., Liu, Y., Ding, Y. F., Yang, C. Y., Yao, Z. F., ... & Pei, J. (2020). *The critical role of dopant cations in electrical conductivity and thermoelectric performance of n-doped polymers.* Journal of the American Chemical Society, 142(36), 15340-15348. https://doi.org/10.1021/jacs.0c05699

Polak, M. P., Scharoch, P., & Kudrawiec, R. (2020). *The effect of isovalent doping on the electronic band structure of group IV semiconductors.* Journal of Physics D: Applied Physics, 54(8), 085102. DOI 10.1088/1361-6463/abc503

Pop, M., & Botiz, I. (2025). Carrier Mobility, Electrical Conductivity, and Photovoltaic Properties of Ordered Nanostructures Assembled from Semiconducting Polymers. *Materials*, *18*(19), 4580.

Rahman, M. H., & Mannodi-Kanakkithodi, A. (2025). Defect modeling in semiconductors: the role of first principles simulations and machine learning. *Journal of Physics: Materials*, *8*(2), 022001.

Roccaforte, F., Giannazzo, F., & Greco, G. (2022). *Ion Implantation Doping in Silicon Carbide and Gallium Nitride Electronic Devices*. Micro, 2(1), 23-53. https://doi.org/10.3390/micro2010002

Sio, H. C., & MacDonald, D. (2016). Direct comparison of the electrical properties of multicrystalline silicon materials for solar cells: conventional p-type, n-type and high performance p-type. *Solar Energy Materials and Solar Cells*, *144*, 339-346.

Wang, C., Chen, C., Kong, W., Wang, H., & Zhou, Z. (2025, August). Multi-parameter Degradation Modeling Method for Power MOSFETs Integrating Semiconductor Physics Degradation Data. In *2025 IEEE Workshop on Wide Bandgap Power Devices and Applications in Asia (WiPDA Asia)* (pp. 1-5). IEEE.

Zhang, J., Wang, J., Li, J., Debnath, T., Zhou, R., Wang, Z., ... & Wu, T. (2023). *Atomic-Level Insights into Manganese-Environment-Related Photophysical Properties of II–III–VI Quantum Dots Using Well-Defined Nanofragments.* The Journal of Physical Chemistry C, 127(32), 15951-15961. https://doi.org/10.1021/acs.jpcc.3c03940